ACS OMEGA

http://pubs.acs.org/journal/acsodf

Article

Network Pharmacology-Based Dissection of the Active Ingredients and Protective Mechanism of the *Salvia Miltiorrhiza* and *Panax Notoginseng* Herb Pair against Insulin Resistance

Xin-Yu Yang, Wen-Xiao Wang, Yu-Xi Huang, Shi-Jun Yue,* Bai-Yang Zhang, Huan Gao, Lei Zhang, Dan Yan, and Yu-Ping Tang*

Cite This: *ACS Omega* 2021, 6, 17276−17288

Read Online

ACCESS | Metrics & More | Article Recommendations | Supporting Information

ABSTRACT: The *Salvia miltiorrhiza* and *Panax notoginseng* herb pair (DQ) has been widely utilized in traditional Chinese medicine for the longevity and for preventing and treating cardio-cerebrovascular diseases. Often associated with cardio-cerebrovascular diseases are comorbidities such as insulin resistance. However, the protective mechanisms of DQ against insulin resistance remain not well understood. Through network pharmacology analysis, a total of 94 candidate active compounds selected from DQ (61 from *S. miltiorrhiza* Bunge and 33 from *P. notoginseng* (Burk.) F. H. Chen) interacted with 52 corresponding insulin resistance-related targets, which mainly involved insulin resistance and the AMPK signaling pathway. Furthermore, the contribution index calculation results indicated 25 compounds as the principal components of this herb pair against insulin resistance. Among them, ginsenoside F2, protocatechuic acid, and salvianolic acid B were selected and validated to promote glucose consumption through activating AMPK phosphorylation and upregulating GLUT4 in insulin-resistant cell model (HepG2/IR) cells. These findings indicated that DQ has the potential for repositioning in the treatment of insulin resistance mainly through the AMPK signaling pathway.

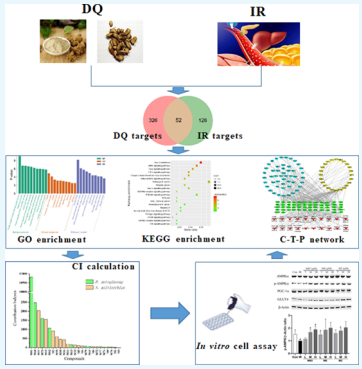

INTRODUCTION

Cardiometabolic diseases have become a worldwide epidemic, mainly because of the dramatically increasing related cardiovascular risk factors such as obesity, type 2 diabetes, nonalcoholic fatty liver disease, atherosclerosis, and hypertension. Often a comorbidity associated with cardiometabolic disease is insulin resistance,[1] which can cause a decline in the efficiency of cellular uptake of glucose, leading to cellular glycolipid metabolism dysfunction.[2] Nowadays, traditional Chinese medicine (TCM) has been widely used in prevention and treatment of cardiometabolic diseases due to their exact curative effects and less side effects.[3] Many clinic prescriptions for the treatment of cardiovascular diseases commonly encompass the *Salvia miltiorrhiza* and *Panax notoginseng* herb pair (DQ), such as Danqi Pills, Compound Danshen Tablets, etc. DQ, activating blood circulation and removing blood stasis,[4] has been discovered to have various beneficial activities such as antihypertensive,[5] anti-inflammatory, and antioxidant effects.[6,7] Additionally, DQ could ameliorate insulin resistance through overall corrective regulation of glycolipid metabolism.[8] Recently, we found that DQ was able to alter peripheral branched-chain amino acid levels of rats with acute myocardial ischemia.[9] Branched-chain amino acids, involved in several pathways of insulin resistance, tend to be increased in peripheral blood of preclinical animal models or individuals with insulin resistance.[10] Therefore, it is particularly interesting to probe the underlying mechanism of DQ against insulin resistance.

Network pharmacology, a holistic and efficient technique, could explore complex interactions between TCM and biological systems from a network perspective.[11] We have successfully applied network pharmacology to interpret the mechanism of actions of herb pairs at the molecular network level.[12,13] In the present study, we tried to establish the compound-target-pathway (C-T-P) network by the network pharmacology model, decipher active ingredients based on the contribution index (CI) calculation, and validate the effects of active components on the insulin-resistant cell model (HepG2/IR) so as to uncover the underlying mechanisms of DQ for treating insulin resistance.

RESULTS

Candidate Active Ingredients in DQ. In the present work, 310 ingredients were retrieved for *S. miltiorrhiza* Bunge (192)

Received: March 5, 2021
Accepted: June 23, 2021
Published: June 30, 2021

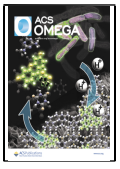

Table 1. Active Ingredients of the *Salvia Miltiorrhiza* and *Panax Notoginseng* Herb Pair

No.	Name	Herb	Degree	No.	Name	Herb	Degree
M1	Salvianolic acid A*	*S. miltiorrhiza* Bunge	3	M48	1,2,5,6-Tetrahydrotanshinone	*S. miltiorrhiza* Bunge	/
M2	Salvianolic acid B*	*S. miltiorrhiza* Bunge	2	M49	Poriferasterol	*S. miltiorrhiza* Bunge	1
M3	Salvianolic acid C*	*S. miltiorrhiza* Bunge	8	M50	Poriferast-5-en-3beta-ol	*S. miltiorrhiza* Bunge	1
M4	Caffeic acid*	*S. miltiorrhiza* Bunge	1	M51	Isoimperatorin	*S. miltiorrhiza* Bunge	2
M5	Rosmarinic acid*	*S. miltiorrhiza* Bunge	11	M52	α-Amyrin	*S. miltiorrhiza* Bunge	1
M6	Protocatechuic acid*	*S. miltiorrhiza* Bunge	2	M53	(+)-Ferruginol	*S. miltiorrhiza* Bunge	/
M7	Protocatechuic aldehyde	*S. miltiorrhiza* Bunge	/	M54	Manool	*S. miltiorrhiza* Bunge	/
M8	Tournefolic acid A	*S. miltiorrhiza* Bunge	/	M55	Microstegiol	*S. miltiorrhiza* Bunge	/
M9	Prolithospermic acid	*S. miltiorrhiza* Bunge	5	M56	Miltipolone	*S. miltiorrhiza* Bunge	1
M10	Tanshinone I	*S. miltiorrhiza* Bunge	2	M57	3-Beta-hydroxymethyllenetanshiquinone	*S. miltiorrhiza* Bunge	2
M11	Tanshinone IIA	*S. miltiorrhiza* Bunge	7	M58	Methylenetanshinquinone	*S. miltiorrhiza* Bunge	2
M12	Tanshinone IIB	*S. miltiorrhiza* Bunge	/	M59	Przewalskin b	*S. miltiorrhiza* Bunge	2
M13	Cryptotanshinone	*S. miltiorrhiza* Bunge	7	M60	2-Isopropyl-8-methylphenanthrene-3,4-dione	*S. miltiorrhiza* Bunge	6
M14	Danshensu*	*S. miltiorrhiza* Bunge	2	M61	4-Methylenemiltirone	*S. miltiorrhiza* Bunge	5
M15	Deoxyneocryptotanshinone	*S. miltiorrhiza* Bunge	4	M62	Ginsenoside Rb1*	*P. notoginseng* (Burk.) F. H. Chen	2
M16	Dihydrotanshinone I	*S. miltiorrhiza* Bunge	3	M63	Ginsenoside Re*	*P. notoginseng* (Burk.) F. H. Chen	2
M17	Epidanshenspiroketallactone	*S. miltiorrhiza* Bunge	4	M64	Ginsenoside F1*	*P. notoginseng* (Burk.) F. H. Chen	/
M18	Isocryptotanshinone	*S. miltiorrhiza* Bunge	4	M65	Ginsenoside F2	*P. notoginseng* (Burk.) F. H. Chen	1
M19	Isotanshinone II	*S. miltiorrhiza* Bunge	4	M66	Ginsenoside Rh1	*P. notoginseng* (Burk.) F. H. Chen	/

https://doi.org/10.1021/acsomega.1c01209
ACS Omega 2021, 6, 17276−17288

Table 1. continued

M20	Nortanshinone	*S. miltiorrhiza* Bunge	2	M67	Ginsenoside Rh2	*P. notoginseng* (Burk.) F. H. Chen	/
M21	Salviolone	*S. miltiorrhiza* Bunge	2	M68	Ginsenoside Rg1	*P. notoginseng* (Burk.) F. H. Chen	5
M22	Dihydrotanshinlactone	*S. miltiorrhiza* Bunge	5	M69	Ginsenoside Rg2	*P. notoginseng* (Burk.) F. H. Chen	1
M23	Dehydrotanshinone II A	*S. miltiorrhiza* Bunge	4	M70	20(R)-Ginsenoside-Rg2	*P. notoginseng* (Burk.) F. H. Chen	/
M24	Tanshindiol A	*S. miltiorrhiza* Bunge	/	M71	20(S)-Ginsenoside-Rg2	*P. notoginseng* (Burk.) F. H. Chen	/
M25	Tanshindiol B	*S. miltiorrhiza* Bunge	1	M72	Ginsenoside Rg3*	*P. notoginseng* (Burk.) F. H. Chen	2
M26	Tanshindiol C	*S. miltiorrhiza* Bunge	/	M73	Ginsenoside Rd	*P. notoginseng* (Burk.) F. H. Chen	2
M27	Tanshinone VI	*S. miltiorrhiza* Bunge	4	M74	Ginsenoside Rc*	*P. notoginseng* (Burk.) F. H. Chen	3
M28	Danshenspiroketallactone	*S. miltiorrhiza* Bunge	3	M75	Ginsenoside Rb2*	*P. notoginseng* (Burk.) F. H. Chen	4
M29	Neocryptotanshinone II	*S. miltiorrhiza* Bunge	5	M76	Ginsenoside Rb3*	*P. notoginseng* (Burk.) F. H. Chen	2
M30	Formyltanshinone	*S. miltiorrhiza* Bunge	1	M77	Ginsenoside Rf*	*P. notoginseng* (Burk.) F. H. Chen	1
M31	1-Ketoisocryptotanshinone*	*S. miltiorrhiza* Bunge	5	M78	Notoginsenoside R1*	*P. notoginseng* (Burk.) F. H. Chen	/
M32	Neocryptotanshinone	*S. miltiorrhiza* Bunge	5	M79	Notoginsenoside R2*	*P. notoginseng* (Burk.) F. H. Chen	1
M33	Miltirone	*S. miltiorrhiza* Bunge	4	M80	Notoginsenoside K*	*P. notoginseng* (Burk.) F. H. Chen	1
M34	Miltionone Ⅰ	*S. miltiorrhiza* Bunge	4	M81	Dencichine*	*P. notoginseng* (Burk.) F. H. Chen	4
M35	Miltionone Ⅱ	*S. miltiorrhiza* Bunge	2	M82	Quercetin	*P. notoginseng* (Burk.) F. H. Chen	27

https://doi.org/10.1021/acsomega.1c01209
ACS Omega 2021, 6, 17276−17288

Table 1. continued

M36	Salviol*	*S. miltiorrhiza* Bunge	2	M83	Lutein*	*P. notoginseng* (Burk.) F. H. Chen	2
M37	Sclareol	*S. miltiorrhiza* Bunge	/	M84	Trilinolein*	*P. notoginseng* (Burk.) F. H. Chen	3
M38	Luteolin	*S. miltiorrhiza* Bunge	12	M85	Liquiritigenin	*P. notoginseng* (Burk.) F. H. Chen	3
M39	(+)-Sugiol	*S. miltiorrhiza* Bunge	/	M86	Diisooctyl phthalate	*P. notoginseng* (Burk.) F. H. Chen	1
M40	Tanshinaldehyde	*S. miltiorrhiza* Bunge	1	M87	Beta-sitosterol	*P. notoginseng* (Burk.) F. H. Chen	5
M41	Baicalin	*S. miltiorrhiza* Bunge	5	M88	Stigmasterol	*P. notoginseng* (Burk.) F. H. Chen	3
M42	Przewaquinone B	*S. miltiorrhiza* Bunge	1	M89	Mandenol	*P. notoginseng* (Burk.) F. H. Chen	/
M43	Przewaquinone C	*S. miltiorrhiza* Bunge	1	M90	Sanchinan-A*	*P. notoginseng* (Burk.) F. H. Chen	1
M44	Danshenol A	*S. miltiorrhiza* Bunge	/	M91	Gypenoside IX	*P. notoginseng* (Burk.) F. H. Chen	1
M45	Danshenol B	*S. miltiorrhiza* Bunge	3	M92	Gypenoside XVII	*P. notoginseng* (Burk.) F. H. Chen	/
M46	Salvilenone	*S. miltiorrhiza* Bunge	/	M93	Protopanaxadiol	*P. notoginseng* (Burk.) F. H. Chen	10
M47	Dan-shexinkum d	*S. miltiorrhiza* Bunge	6	M94	Protopanaxatriol*	*P. notoginseng* (Burk.) F. H. Chen	12

[a]Compounds with OB < 30% and/or DL < 0.18, yet validated pharmaceutically.

and *P. notoginseng* (Burk.) F. H. Chen (118), which are provided in Table S1. Oral bioavailability (OB) and drug-likeness (DL) were employed to screen the candidate active ingredients from DQ. A few compounds that do not meet either of these two criteria were also selected in the cases of high bioactivities and huge amounts. Consequently, a total of 94 candidate active compounds (mainly phenolic acids, phenanthrenequinones, and saponins) were selected from DQ (61 from *S. miltiorrhiza* Bunge and 33 from *P. notoginseng* (Burk.) F. H. Chen) (Table 1).

Potential Targets of DQ against Insulin Resistance. A total of 376 corresponding targets of 94 candidate active compounds in DQ were obtained from TCM Systems Pharmacology Database and Analysis Platform (TCMSP) and SwissTargetPrediction. Then, 178 targets related to insulin resistance were retrieved from Comparative Toxicogenomics Database (CTD), GeneCards, and Online Mendelian Inheritance in Man (OMIM). By matching these two target clusters by a Venn diagram, 52 overlapped targets were selected as the potential targets of DQ against insulin resistance (Figure 1 and Table 2).

Gene Ontology (GO) Enrichment and Kyoto Encyclopedia of Genes and Genomes (KEGG) Pathway Analysis.

Figure 1. Venn diagram showing the numbers of the overlapped and specific targets among the *Salvia miltiorrhiza* and *Panax notoginseng* herb pair (pink circle) and insulin resistance (green circle).

https://doi.org/10.1021/acsomega.1c01209
ACS Omega 2021, 6, 17276−17288

Table 2. Insulin-Resistant Targets of the *Salvia Miltiorrhiza* and *Panax Notoginseng* Herb Pair

ID	Target	UniProt ID	Gene name	Degree
T1	Caspase-1	P29466	CASP1	3
T2	G1/S-specific cyclin-D1	P24385	CCND1	12
T3	Nuclear receptor subfamily 1 group I member 3	Q14994	NR1I3	3
T4	DNA topoisomerase 2-alpha	P11388	TOP2A	2
T5	Inhibitor of nuclear factor kappa-B kinase subunit beta	O14920	IKBKB	16
T6	Tumor necrosis factor	P01375	TNF	17
T7	Sterol regulatory element-binding protein 2	Q12772	SREBF2	2
T8	Heme oxygenase 1	P09601	HMOX1	3
T9	Nitric oxide synthase, inducible	P35228	NOS2	13
T10	Interleukin-6	P05231	IL6	14
T11	Insulin-like growth factor-binding protein 3	P15473	IGFBP3	1
T12	Caveolin-1	Q03135	CAV1	2
T13	Androgen receptor	P10275	AR	26
T14	Eotaxin	P51671	CCL11	1
T15	Nitric oxide synthase, endothelial	P29474	NOS3	12
T16	Corticosteroid 11-beta-dehydrogenase isozyme 1	P28845	HSD11B1	9
T17	Peroxisome proliferator-activated receptor gamma	P37231	PPARG	24
T18	Insulin receptor	P06213	INSR	11
T19	Complement C3	P01024	C3	3
T20	Peroxisome proliferator-activated receptor alpha	Q07869	PPARA	4
T21	Proto-oncogene c-Fos	P01100	FOS	9
T22	Progesterone receptor	P06401	PGR	8
T23	Aryl hydrocarbon receptor	P35869	AHR	1
T24	C-C motif chemokine 2	P13500	CCL2	5
T25	Fatty acid synthase	P49327	FASN	4
T26	Nuclear receptor subfamily 1 group I member 2	O75469	NR1I2	3
T27	Endothelin-1 receptor	P25101	EDNRA	2

https://doi.org/10.1021/acsomega.1c01209
ACS Omega 2021, 6, 17276−17288

Table 2. continued

T28	Natriuretic peptides A	P01160	NPPA	2
T29	Insulin-like growth factor II	P01344	IGF2	2
T30	C-reactive protein	P02741	CRP	1
T31	Tyrosine-protein phosphatase non-receptor type 1	P18031	PTPN1	6
T32	Calcium/calmodulin-dependent protein kinase kinase 2	Q96RR4	CAMKK2	8
T33	C-C chemokine receptor type 2	P41597	CCR2	1
T34	Insulin-like growth factor 1 receptor	P08069	IGF1R	8
T35	Acetyl-CoA carboxylase 1	Q13085	ACACA	3
T36	Beta-2 adrenergic receptor	P07550	ADRB2	31
T37	Estrogen receptor	P03372	ESR1	25
T38	Solute carrier family 2, facilitated glucose transporter member 4	P14672	SLC2A4	8
T39	Heat shock protein HSP 90	P08238	HSP90AB1	23
T40	Glucocorticoid receptor	P04150	NR3C1	4
T41	Serum paraoxonase/arylesterase 1	P27169	PON1	2
T42	5'-AMP-activated protein kinase catalytic subunit alpha-2	P54646	AMPK	16
T43	Acetyl-CoA carboxylase 2	O00763	ACACB	5
T44	E3 ubiquitin-protein ligase XIAP	P98170	XIAP	3
T45	Sex hormone-binding globulin	P04278	SHBG	2
T46	C-C motif chemokine 3	P10147	CCL3	3
T47	Phosphatidylinositol-3,4,5-trisphosphate 3-phosphatase and dual-specificity protein phosphatase PTEN	P60484	PTEN	9

https://doi.org/10.1021/acsomega.1c01209
ACS Omega 2021, 6, 17276−17288

Table 2. continued

T48	Epidermal growth factor receptor	P00533	EGFR	9
T49	5-Hydroxytryptamine 2C receptor	P28335	HTR2C	2
T50	RAC-alpha serine/threonine-protein kinase	P31749	AKT1	26
T51	Lysosomal alpha-glucosidase	P10253	GAA	2
T52	Solute carrier family 2, facilitated glucose transporter member 4	P14672	GLUT4	10

The top 10 significantly enriched terms with a greater number of involved targets in biological process (BP), molecular function (MF), and cellular component (CC) categories ($P < 0.05$, P-values were corrected using the Benjamini-Hochberg procedure) are shown in Figure 2A, indicating that DQ may regulate the response to hypoxia, inflammatory response, ERK1 and ERK2 cascades, and nitric oxide biosynthetic processes via nitric oxide synthase regulator activity, RNA polymerase II transcription factor activity, and enzyme binding in the cytosol, caveola, and perinuclear region of the cytoplasm so as to exert insulin resistance-alleviating potential. The top 10 significantly enriched KEGG pathways are listed in Figure 2B, suggesting that DQ may alleviate insulin resistance mainly through the AMPK signaling pathway, FoxO signaling pathway, HIF-1 signaling pathway, and adipocytokine signaling pathway. Particularly, the HIF-1 signaling pathway and FoxO signaling pathway are mainly associated with diabetic retinopathy and diabetic nephropathy, respectively, suggesting that DQ has the capacity to treat diabetic complications. Also, DQ could regulate inflammation-related pathways (such as the TNF signaling pathway, Toll-like receptor signaling pathway, and NOD-like receptor signaling pathway). Actually, chronic inflammation is one of the main causes of insulin resistance.[14] Since insulin is the primary hormonal mediator of tumor metabolism and growth in obesity-associated insulin resistance,[15] cancer related pathways were highly enriched in our study, suggestive of the anticancer potential of DQ.

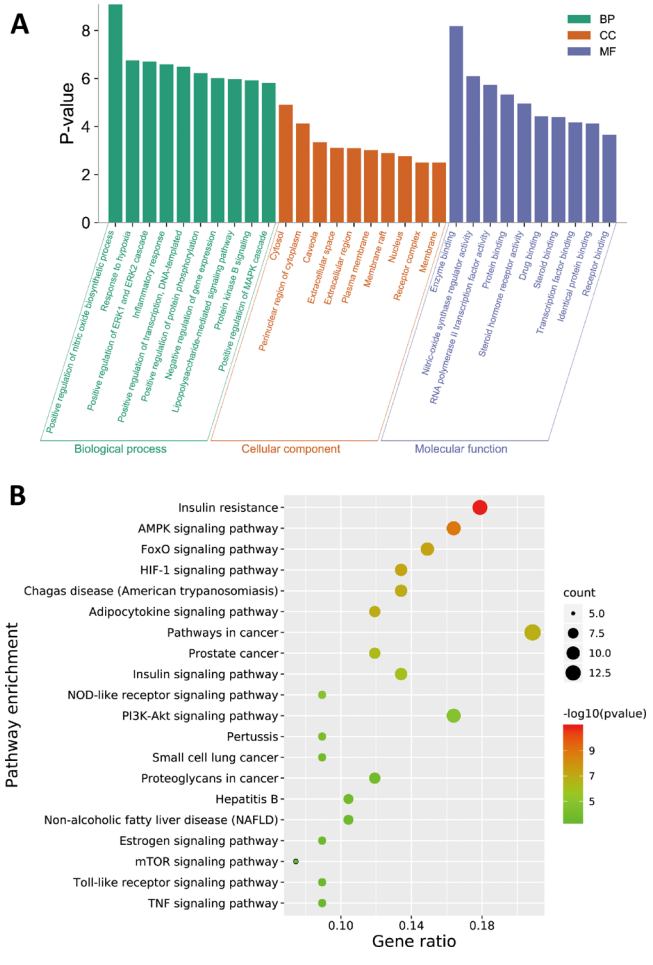

Figure 2. GO enrichment (A) and KEGG pathway (B) analysis of the insulin-resistant targets of the *Salvia miltiorrhiza* and *Panax notoginseng* herb pair.

C-T-P Network Analysis and CI Calculation. A global view of the C-T-P network was generated by Cytoscape 3.8.0, which consisted of 145 nodes (73 ingredients, 52 targets, and 20 pathways) and 431 edges (Figure 3). Most targets were shared by candidate active compounds in both herbs. These candidate

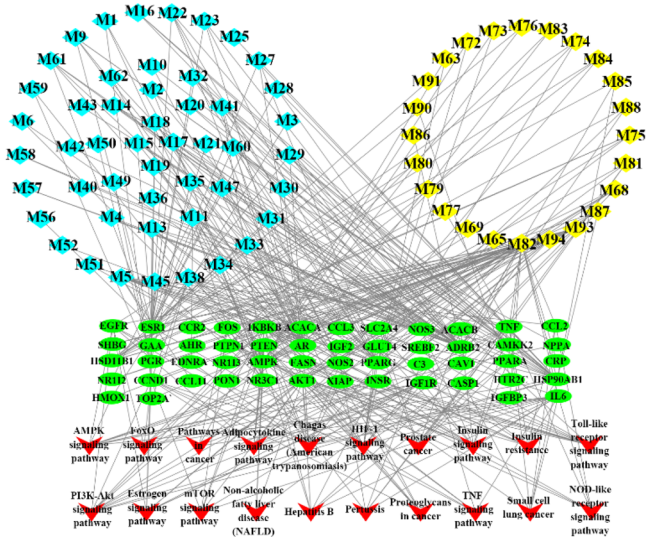

Figure 3. Compound-target-pathway network of the *Salvia miltiorrhiza* and *Panax notoginseng* herb pair against insulin resistance. The light blue and yellow nodes are active ingredients of *S. miltiorrhiza* and *P. notoginseng*, respectively. The light green nodes are the potential targets, while the red nodes represent the pathways.

https://doi.org/10.1021/acsomega.1c01209
ACS Omega 2021, 6, 17276−17288

active ingredients with high interconnection degrees were responsible for the high interconnectedness of the C-T-P network, especially quercetin (M82, degree = 27), luteolin (M38, degree = 12), protopanaxatriol (M94, degree = 12), rosmarinic acid (M5, degree = 11), and protopanaxadiol (M93, degree = 10). The majority of the targets such as ADRB2 (degree = 31), AMPK (degree = 26), AKT1 (degree = 26), AR (degree = 26), ESR1 (degree = 25), PPARG (degree = 24), and HSP90AB1 (degree = 23) were mapped onto KEGG pathways associated with glucose and insulin homeostasis.

Based on this network integrating the component content in herbs, a CI of every candidate active ingredient in DQ was proposed (Figure 4 and Tables S2 and S3). Dencichine (M81),

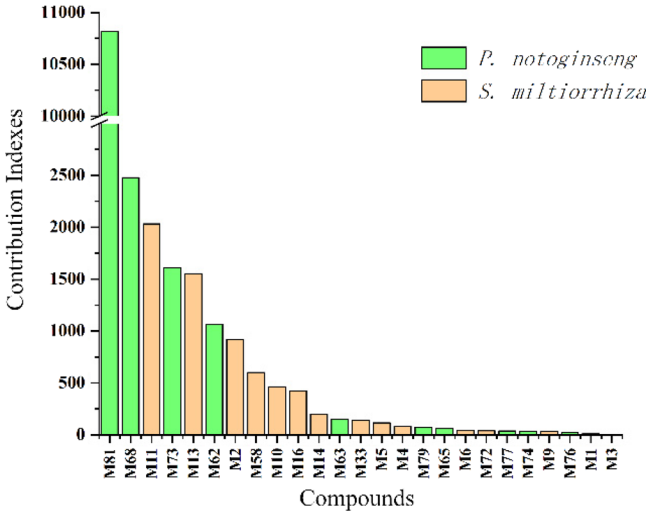

Figure 4. Contribution index of active ingredients (top 25) in the *Salvia miltiorrhiza* and *Panax notoginseng* herb pair against insulin resistance.

ginsenoside Rg1 (M68), tanshinone IIA (M11), ginsenoside Rd (M73), cryptotanshinone (M13), ginsenoside Rb1 (M62), salvianolic acid B (M2), methylenetanshinquinone (M58), tanshinone I (M10), and dihydrotanshinone I (M16) were ranked as the top 10 active ingredients according to CI calculation, which displayed the most contribution to the insulin resistance-alleviating effect of DQ.

Cytotoxicity of Active Ingredients of DQ on HepG2 Cells. Among 25 active compounds shown in Figure 4, the cytotoxicity of 21 commercially available active ingredients in DQ on HepG2 cells was evaluated by Cell Counting Kit-8 (CCK-8) assay. The results showed a survival rate of ≤85% for all the concentrations tested of tanshinone I, tanshinone IIA, cryptotanshinone, and dihydrotanshinone I, indicating that these compounds possess certain cytotoxicity on HepG2 cells (Figure S1), which were consistent with the previous study.[16] Furthermore, 14 active ingredients of DQ with a survival rate of ≥90% for all the concentrations tested were selected for further study (Figure S1).

Glucose Consumption and AMPK Expression in HepG2/IR Cells by Active Ingredients of DQ. As shown in Figure 5, salvianolic acid A (M1), rosmarinic acid, danshensu (M14), ginsenoside Rc (M74), and ginsenoside Rb3 (M76) tested at three concentrations did not increase glucose consumption in HepG2/IR cells, whereas other ingredients including caffeic acid (M4), ginsenoside Rd, and dencichine could increase glucose consumption to varying degrees. Notably, salvianolic acid B, protocatechuic acid (M6), ginsenoside Rb1, ginsenoside Re (M63), ginsenoside F2 (M65), and ginsenoside Rf (M77) increased glucose consumption concentration-dependently in HepG2/IR cells.

Recently, numerous studies indicated that the activation of AMPK in the liver, skeleton muscle, and adipose tissue promotes glucose consumption, insulin sensitivity, fatty acid oxidation, and mitochondrial biogenesis.[17] To reveal whether active ingredients of DQ regulate hepatic glucose metabolism via the AMPK signaling pathway, we measured the phosphorylation of AMPK, which is required for AMPK activation. Since ginsenoside Rb1, ginsenoside Re, and ginsenoside Rf were well studied,[18−21] salvianolic acid B, protocatechuic acid, and ginsenoside F2 were chosen to determine their roles in the AMPK signaling pathway in HepG2/IR cells. As demonstrated in Figure 6, these three compounds activated AMPK activity by inducing the phosphorylation of AMPK significantly in HepG2/IR cells, whereas the expression of AMPK and PGC-1α was not significantly influenced. Since defective GLUT4 transport is a feature of insulin resistance,[22] we have also investigated the effects of these three ingredients on GLUT4. As shown in Figure 6E, GLUT4 protein expression in the insulin resistance group was significantly reduced compared with the control group ($P < 0.01$). These three ingredients were able to significantly increase the expression of GLUT4 protein at certain concentrations ($P < 0.05$ or $P < 0.01$).

DISCUSSION

Insulin resistance is one of the most important factors of cardiometabolic diseases, which greatly threaten global pop-

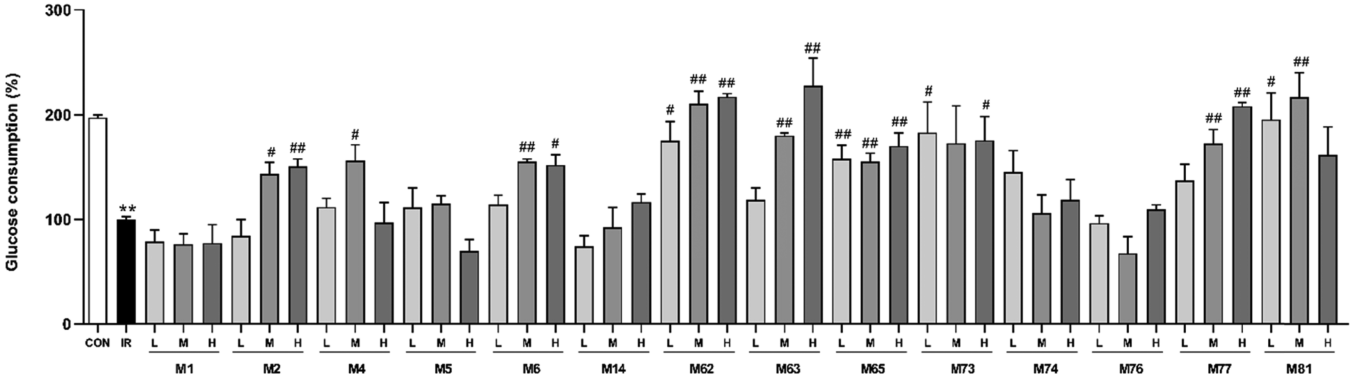

Figure 5. Glucose consumption in HepG2/IR cells by active ingredients of the *Salvia miltiorrhiza* and *Panax notoginseng* herb pair. Data were expressed as mean ± SD ($n = 3$). $^{**}P < 0.01$ versus the control (Con) group; $^{\#}P < 0.05$, $^{\#\#}P < 0.01$ versus the insulin resistance (IR) group.

https://doi.org/10.1021/acsomega.1c01209
ACS Omega 2021, 6, 17276−17288

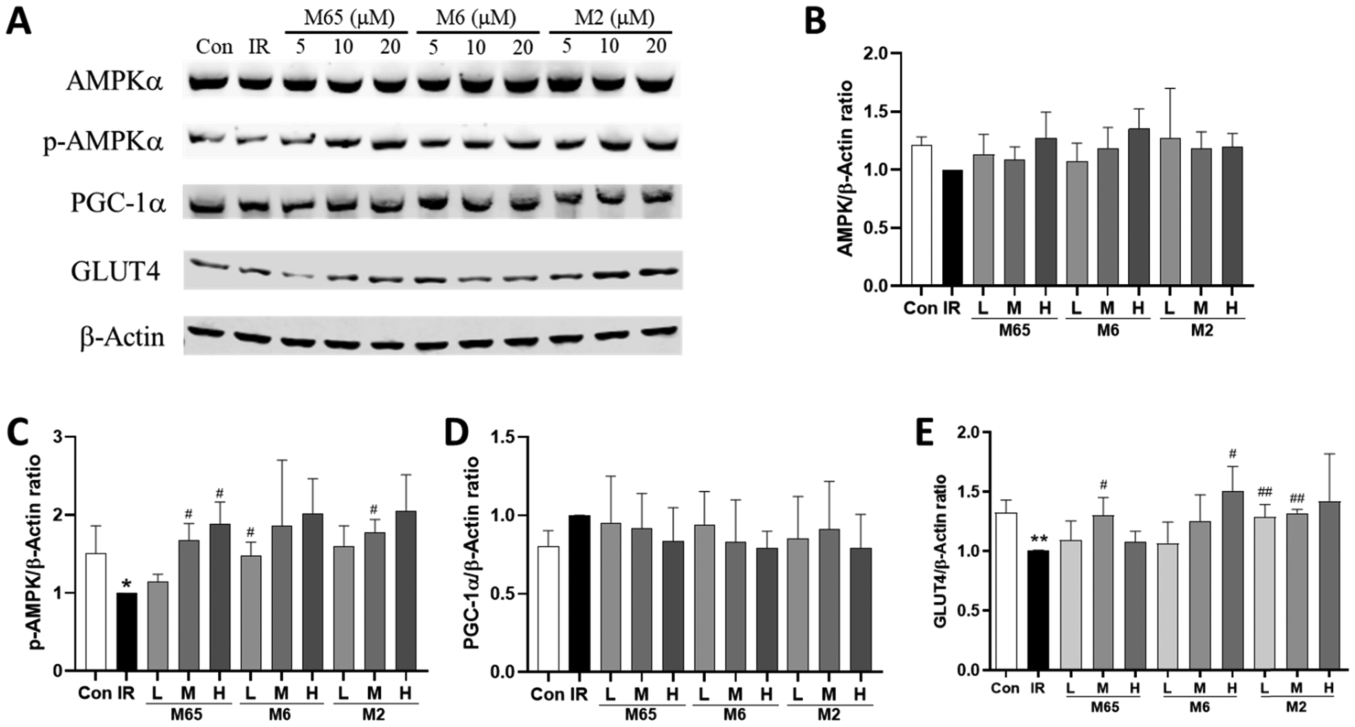

Figure 6. Effects of active ingredients of the *Salvia miltiorrhiza* and *Panax notoginseng* herb pair on AMPK, p-AMPK, PGC-1α, and GLUT4 protein expression in HepG2/IR cells. (A) Bands of AMPK, p-AMPK, PGC-1α, and GLUT4. β-Actin was used as the loading control. Protein expression levels of AMPK (B), p-AMPK (C), PGC-1α (D), and GLUT4 (E). Data were expressed as mean ± SD (n = 3). *P < 0.05 versus the control (Con) group; $^{\#}P$ < 0.05 versus the insulin resistance (IR) group.

ulation health. Either *S. miltiorrhiza* Bunge or *P. notoginseng* (Burk.) F. H. Chen is useful for preserving insulin homeostasis.[23,24] However, the protective mechanisms of their combination-DQ against insulin resistance remain not well understood. In this study, an integrated network pharmacology approach was successfully applied to illuminate the molecular mechanism of DQ on insulin resistance. Ninety-four candidate active ingredients and 52 corresponding insulin resistance-related targets were selected and predicted, which were largely involved in multiple biological processes and pathways associated with the therapy and prophylaxis of insulin resistance. For a better understanding of the core components and pharmacological mechanism of DQ, we introduced a new parameter, CI, to mimic the compatible combination of all the active components in DQ from the perspective of both intrinsic properties and importance in a network. Specifically, CI is the product of proportion of herbs in DQ, content of each component in a relative herb, the oral bioavailability of each component, and the rank sum ratio (RSR) of integrated network topology parameters. Therefore, the ranked order of CI of each component can be considered as the extent of how much a component is involved in the pharmacological mechanism of DQ against insulin resistance. Therefore, from the C-T-P network together with CI calculations, it is reasonable that *S. miltiorrhiza* and *P. notoginseng* are usually used in combination exerting synergistic and complementary therapeutic actions.

Among the top 25 active ingredients based on CI calculations, 9 were shown to increase glucose consumption in HepG2/IR cells to varying degrees with no obvious cytotoxicity. As a major regulator of cellular energy homeostasis, AMPK plays a critical role in the regulation of peripheral glucose levels and is believed to be a therapeutic target of obesity and type 2 diabetes.[25] The development of cardiometabolic disorders is closely related to the improper function of the energy regulating network, including AMPK and PGC-1α.[26] Therefore, salvianolic acid B, protocatechuic acid, and ginsenoside F2 were further chosen and proven to activate AMPK activity by inducing the phosphorylation of AMPK significantly in HepG2/IR cells without influencing PGC-1α, so as to alleviate insulin resistance. It has found that a ginsenoside F2-enriched mixture improved nonalcoholic fatty liver disease via its antioxidant effects and activation of AMPK.[27] Protocatechuic acid improved glucose tolerance and insulin sensitivity in obese mice via activating the AMPK/mTOR/S6K pathway.[28] Salvianolic acid B ameliorated hyperglycemia in db/db mice through the AMPK pathway.[29] In this study, our findings were well corroborated with these previous in vivo results. Notably, as shown in Figure S2, these three ingredients could not only increase glucose consumption to varying degrees in palmitic acid-induced insulin-resistant HepG2 cells but also increase the phosphorylation level of Akt and the ratio of p-Akt/Akt, suggestive of the huge potential to be insulin resistance-alleviating agents. It must be mentioned that salvianolic acid A, rosmarinic acid, ginsenoside Rb3, and ginsenoside Rc did not increase glucose consumption in HepG2/IR cells in our study, which were in contradiction with previous studies.[30−33] The key reason of this paradox is the different concentrations of compounds tested. For instance, rosmarinic acid and ginsenoside Rb3 promoted glucose utilization of HepG2/IR cells in a dose-dependent manner, which were statistically significant from 25 μM,[31,32] whereas only 5, 10, and 20 μmol/L rosmarinic acid and ginsenoside Rb3 were tested in our study. Since major tanshinones from *S. miltiorrhiza* Bunge exhibit obvious cytotoxic effects based on our findings as well as previous studies,[16] phenolic acids and saponins may be mainly responsible for the insulin resistance-alleviating effect of DQ.

https://doi.org/10.1021/acsomega.1c01209
ACS Omega 2021, 6, 17276−17288

CONCLUSIONS

In this study, a systematical network pharmacology approach was constructed to evaluate DQ for treating insulin resistance. A total of 94 candidate active compounds selected from DQ interacted with 52 corresponding insulin resistance-related targets, which mainly involved insulin resistance and the AMPK signaling pathway. The CI calculation showed 25 compounds as the principal components of DQ against insulin resistance. Furthermore, ginsenoside F2, protocatechuic acid, and salvianolic acid B were validated to promote glucose consumption through activating AMPK phosphorylation in HepG2/IR cells. Our results provide a theoretical basis for the potential of DQ for repositioning in the treatment of insulin resistance.

MATERIALS AND METHODS

Active Ingredient Screening. All the ingredient data of *S. miltiorrhiza* Bunge and *P. notoginseng* (Burk.) F. H. Chen were retrieved from TCMSP (https://tcmspw.com/tcmsp.php)[34] and then manually supplemented through a wide-scale text-mining method. The candidate active ingredients from two herbs were mainly filtered by integrating oral bioavailability (OB $\geq$ 30%) and drug-likeness (DL $\geq$ 0.18).[35,36] Other compounds with profound pharmacological effects and high contents were also kept.

Target Prediction. All candidate active ingredients of DQ were imported into TCMSP to obtain targets. These ingredients with less targets were further introduced into the SwissTargetPrediction (http://www.swisstargetprediction.ch/) to seek targets (probability > 0.02).[37] The target information of insulin resistance was collected from CTD (http://ctdbase.org/),[38] OMIM database (http://www.omim.org/),[39] and GeneCards (https://www.genecards.org/),[40] respectively. The overlapped targets (only *Homo sapiens*) between candidate active ingredients and insulin resistance were finally chosen as the insulin resistance-related targets of DQ.

GO and KEGG Pathway Analysis. The Database for Annotation, Visualization, and Integrated Discovery (DAVID 6.8, https://david.ncifcrf.gov/) web server was employed to perform GO and KEGG pathway enrichment analysis for the insulin resistance-related targets of DQ.[41]

Network Construction. The C-T-P network of DQ was generated and analyzed by Cytoscape 3.8.0 (http://www.cytoscape.org/), an open-source software package project for visualizing, integrating, modeling, and analyzing the interaction networks.[42]

CI Calculation. In order to screen active ingredients to the insulin resistance-alleviating effect of DQ, a novel CI based on both the intrinsic properties (content) of active components in the corresponding herb and the importance of active components in the disease regulatory network (RSR: the rank sum ratio of integrated network topology parameters) was proposed, which was strongly motivated by the previously published approach,[43,44] as follows:

$$CI_{i,j} = \frac{m_i}{\sum_i^n m_i} \times \frac{C_{i,j}}{M_j} \times OB_j \times \mathrm{RSR}_j \times 10^7$$

where $CI_{i,j}$ is the CI of component j in herb i, m_i is the weight of herb i in DQ, n is the total count of herbs in DQ (since there is no available information, the dose and ratio of the individual herb in DQ are not considered in the current study), $C_{i,j}$ is the content of component j in herb i, M_j is the molecular weight of component j, OB_j represented the oral bioavailability of compound j retrieved from the TCMSP database, and RSR_j is the rank sum ratio of component j in the C-T-P network, which calculated from network topology parameters including Degree, Betweenness, Closeness, Eccentricity, Neighborhood connectivity, and Average Shortest Path Length.

Cell Culture. The HepG2 cells were obtained from American Type Cell Culture Collection (ATCC, Manassas, VA, USA). The cells were cultured in Dulbecco's Modified Eagle Medium (DMEM, Macgene, Beijing, China). All culture medium contains 10% fetal bovine serum (FBS, Bioind, Israel), 100 units/mL penicillin (Invitrogen, Carlsbad, CA, USA), and 100 mg/mL streptomycin (Invitrogen, Carlsbad, CA, USA) in 5% CO_2 in a humidified atmosphere. In all experiments, the cells were cultured to reach 70−80% confluence.

Cell Viability Assay. The HepG2 cells (1×10^4) were seeded in 96-well plates and the medium was removed after 24 h. The cells with different active ingredients of DQ (Table S4) at various concentrations (0, 5, 10, 20, and 40 μmol/L), dissolved in DMEM with FBS deprivation to a total volume of 200 μL/well and cultured at 37 °C in a 5% CO_2 humidified atmosphere for 24 h. Then, 10 μL CCK-8 (DOJINDO, Kyushu, Japan) was added to 90 μL DMEM of each well followed by 2 h of incubation at 37 °C. Absorbance was measured at 450 nm. The cell viability rate was calculated as follows: the OD value of the experimental group/the OD value of the nondrug group × 100%.

Glucose Consumption Assay. The HepG2 cells were seeded as mentioned above in 96-well plates. After 24 h, the cells were washed two times with PBS and then treated with or without 50 mmol/L D-glucose (Macgene, Beijing, China) DMEM for 24 h to induce insulin resistance.[45] The HepG2/IR cells were treated with different active ingredients of DQ at various concentrations (0, 5, 10, and 20 μmol/L, these doses produced no cytotoxicity in HepG2 cells) for 24 h. The cells were washed three times with PBS and treated with the medium containing 100 nM insulin and DMEM containing 1000 mg/mL D-glucose for 25 min. Glucose content in the supernatant of each well was detected using a glucose oxidase-peroxidase method kit (GOD-POD, APPLYGEN, Beijing, China) and absorbance was measured at 550 nm. A blank control group was set up by the detecting medium. The glucose consumption was calculated as follows: (blank control group glucose content − supernatant glucose content of each group)/(blank control group glucose content − supernatant glucose content of the insulin-resistant group) × 100%.[46]

Analysis of Protein Expression. The HepG2/IR cells were treated with different active ingredients of DQ at various concentrations (5, 10, and 20 μmol/L) for 24 h. Total protein was isolated by using RIPA lysis buffer (Beyotime, Shanghai, China) and protease inhibitor cocktail for general use (Beyotime, Shanghai, China) and centrifuged at 12,000 × g for 20 min at 4 °C. The protein amount was measured using a BCA protein assay reagent (Sigma-Aldrich, USA). After equal amounts of proteins were separated with 10% SDS-PAGE gel, proteins were transferred onto a nitrocellulose blotting membrane (Pall Life Sciences, USA). The membranes were then blocked by 5% fat-free milk for 2 h at room temperature, and incubated, respectively, with AMPK (62 kDa; 1:1000), phospho-AMPK (Thr172) (62 kDa; 1:1000), PGC-1α (130 kDa; 1:1000) (CST, Cambridge, MA, USA), GLUT4 (54 kDa; 1:1000) (Affinity Biosciences, Cincinnati, OH, USA), and β-actin (42 kDa; 1:2000) (Zhongshan Jinqiao, Beijing, China)

https://doi.org/10.1021/acsomega.1c01209
ACS Omega 2021, 6, 17276−17288

antibodies at 4 °C overnight followed by incubation with Alexa Fluor 790 goat anti-rabbit IgG H&L (1:10,000, ab186697, Abcam, Cambridge, UK) or Alexa Fluor 680 goat anti-mouse IgG H&L (1:10,000, ab186694, Abcam, Cambridge, UK). Finally, fluorescence signals were collected using an Odyssey infrared imaging system (LI-COR, Lincoln, NE, USA). Using Photoshop software (Adobe Systems, Inc., CA, USA) densitometric analysis was performed to determine optical density of protein bands and normalized to β-actin expression.

Statistical Analysis. Statistical analysis was accomplished with the Prism 6.0 statistical program (GraphPad). The results were presented as mean ± SD. Statistical variations were analyzed by Student's *t*-test or one-way ANOVA followed by Tukey's post-test, $P < 0.05$ was considered statistically significant.

■ ASSOCIATED CONTENT

Supporting Information

The Supporting Information is available free of charge at https://pubs.acs.org/doi/10.1021/acsomega.1c01209.

The detailed information of all compounds in the *Salvia miltiorrhiza* and *Panax notoginseng* herb pair (Table S1), the Network topology parameters and RSR value of the active compounds in the *Salvia miltiorrhiza* and *Panax notoginseng* herb pair against insulin resistance (Table S2), the weight coefficient of active compounds of the *Salvia miltiorrhiza* and *Panax notoginseng* herb pair against insulin resistance (Table S3), the manufacturer and batch number of active compounds in the *Salvia miltiorrhiza* and *Panax notoginseng* herb pair involved in the in vitro cellular validation (Table S4), the results of the cytotoxicity of active ingredients of the *Salvia miltiorrhiza* and *Panax notoginseng* herb pair on HepG2 cells, the name of active ingredients refers to Table 1 (Figure S1), glucose consumption and western blotting results of AKT, p-AKT, and p-AKT/AKT in palmitic acid-induced insulin-resistant HepG2 cells by active ingredients of the *Salvia miltiorrhiza* and *Panax notoginseng* herb pair (Figure S2) (PDF)

■ AUTHOR INFORMATION

Corresponding Authors

Shi-Jun Yue − *Key Laboratory of Shaanxi Administration of Traditional Chinese Medicine for TCM Compatibility, Shaanxi University of Chinese Medicine, Xi'an 712046, China*; orcid.org/0000-0003-2097-223X; Email: shijun_yue@163.com

Yu-Ping Tang − *Key Laboratory of Shaanxi Administration of Traditional Chinese Medicine for TCM Compatibility, Shaanxi University of Chinese Medicine, Xi'an 712046, China*; orcid.org/0000-0002-1272-057X; Email: yupingtang@sntcm.edu.cn

Authors

Xin-Yu Yang − *Department of Pharmacy, Beijing Key Laboratory of Bio-characteristic Profiling for Evaluation of Rational Drug Use, Beijing Shijitan Hospital, Capital Medical University, Beijing 100038, China*

Wen-Xiao Wang − *Key Laboratory of Shaanxi Administration of Traditional Chinese Medicine for TCM Compatibility, Shaanxi University of Chinese Medicine, Xi'an 712046, China*

Yu-Xi Huang − *Key Laboratory of Shaanxi Administration of Traditional Chinese Medicine for TCM Compatibility, Shaanxi University of Chinese Medicine, Xi'an 712046, China*

Bai-Yang Zhang − *Key Laboratory of Shaanxi Administration of Traditional Chinese Medicine for TCM Compatibility, Shaanxi University of Chinese Medicine, Xi'an 712046, China*

Huan Gao − *Key Laboratory of Shaanxi Administration of Traditional Chinese Medicine for TCM Compatibility, Shaanxi University of Chinese Medicine, Xi'an 712046, China*

Lei Zhang − *Department of Pharmacy, Beijing Key Laboratory of Bio-characteristic Profiling for Evaluation of Rational Drug Use, Beijing Shijitan Hospital, Capital Medical University, Beijing 100038, China*

Dan Yan − *Capital Medical University Affiliated Beijing Friendship Hospital, Beijing 100050, China*

Complete contact information is available at: https://pubs.acs.org/10.1021/acsomega.1c01209

Author Contributions

S-J.Y. and Y-P.T. conceived and proposed the idea. S-J.Y. and W-X.W. designed the study. S-J.Y., Y-X.H., W-X.W., and X-Y.Y. performed the experiments. W-X.W., Y-X.H., B-Y.Z., and L.Z. participated in data analysis. S-J.Y., X-Y.Y., D.Y., and Y-P.T. contributed to writing, revising, and proof-reading the manuscript. All authors reviewed and approved the final manuscript. X.Y., W.W., and Y.H. contributed equally to this work.

Notes

The authors declare no competing financial interest.

■ ACKNOWLEDGMENTS

This work was supported by the National Natural Science Foundation of China (81903786 and 82004011), the Beijing Natural Science Foundation (7194280), the Natural Science Foundation of Shaanxi Province (2019JQ-054), the Young Talent Support Program from the Association for Science and Technology of Colleges in Shaanxi Province (20190306), Shaanxi Administration of Traditional Chinese Medicine (2019-ZZ-JC018), and Open Research Funding of Beijing Key Laboratory of Bio-characteristic Profiling for Evaluation of Rational Drug Use (2020-KF13).

■ REFERENCES

(1) Ormazabal, V.; Nair, S.; Elfeky, O.; Aguayo, C.; Salomon, C.; Zuñiga, F. A. Association between insulin resistance and the development of cardiovascular disease. *Cardiovasc. Diabetol.* **2018**, *17*, 122.

(2) Samuel, V. T.; Shulman, G. I. The pathogenesis of insulin resistance: integrating signaling pathways and substrate flux. *J. Clin. Invest.* **2016**, *126*, 12−22.

(3) Lyu, M.; Wang, Y. F.; Fan, G. W.; Wang, X. Y.; Xu, S. Y.; Zhu, Y. Balancing herbal medicine and functional food for prevention and treatment of cardiometabolic diseases through modulating gut microbiota. *Front. Microbiol.* **2017**, *8*, 2146.

(4) Xiong, X. J.; Wang, Z.; Wang, J. Innovative strategy in treating angina pectoris with Chinese patent medicines by promoting blood circulation and removing blood stasis: experience from combination therapy in Chinese medicine. *Curr. Vasc. Pharmacol.* **2015**, *13*, 540−553.

(5) Baek, E. B.; Yoo, H. Y.; Park, S. J.; Chung, Y. S.; Hong, E. K.; Kim, S. J. Inhibition of arterial myogenic responses by a mixed aqueous extract of *Salvia miltiorrhiza* and *Panax notoginseng* (PASEL) showing antihypertensive effects. *Korean J. Physiol. Pharmacol.* **2009**, *13*, 287−293.

(6) Zhao, G.; Xiang, Z.; Ye, T.; Yuan, Y.; Guo, Z. Antioxidant activities of *Salvia miltiorrhiza* and *Panax notoginseng*. *Food Chem.* **2006**, *99*, 767−774.
(7) Zhou, X.; Razmovski-Naumovski, V.; Kam, A.; Chang, D.; Li, C. G.; Chan, K.; Bensoussan, A. Synergistic study of a Danshen (Salvia Miltiorrhizae Radix et Rhizoma) and Sanqi (Notoginseng Radix et Rhizoma) combination on cell survival in EA.hy926 cells. *BMC Complement. Altern. Med.* **2019**, *19*, 50.
(8) Xie, Z.; Loi Truong, T.; Zhang, P.; Xu, F.; Xu, X.; Li, P. Dan-Qi prescription ameliorates insulin resistance through overall corrective regulation of glucose and fat metabolism. *J. Ethnopharmacol.* **2015**, *172*, 70−79.
(9) Tao, H.; Yang, X.; Wang, W.; Yue, S.; Pu, Z.; Huang, Y.; Shi, X.; Chen, J.; Zhou, G.; Chen, Y.; et al. Regulation of serum lipidomics and amino acid profiles of rats with acute myocardial ischemia by *Salvia miltiorrhiza* and *Panax notoginseng* herb pair. *Phytomedicine* **2020**, *67*, No. 153162.
(10) Yue, S. J.; Liu, J.; Wang, A. T.; Meng, X. T.; Yang, Z. R.; Peng, C.; Guan, H. S.; Wang, C. Y.; Yan, D. Berberine alleviates insulin resistance by reducing peripheral branched-chain amino acids. *Am. J. Physiol. Endocrinol. Metab.* **2019**, *316*, E73−E85.
(11) Yue, S. J.; Liu, J.; Feng, W. W.; Zhang, F. L.; Chen, J. X.; Xin, L. T.; Peng, C.; Guan, H. S.; Wang, C. Y.; Yan, D. System pharmacology-based dissection of the synergistic mechanism of Huangqi and Huanglian for diabetes mellitus. *Front. Pharmacol.* **2017a**, *8*, No. 694.
(12) Yue, S. J.; Liu, J.; Feng, W. W.; Zhang, F. L.; Chen, J. X.; Xin, L. T.; Peng, C.; Guan, H. S.; Wang, C. Y.; Yan, D. System pharmacology-based dissection of the synergistic mechanism of Huangqi and Huanglian for diabetes mellitus. *Front. Pharmacol.* **2017a**, *8*, 694.
(13) Yue, S. J.; Xin, L. T.; Fan, Y. C.; Li, S. J.; Tang, Y. P.; Duan, J. A.; Guan, H. S.; Wang, C. Y. Herb pair Danggui-Honghua: mechanisms underlying blood stasis syndrome by system pharmacology approach. *Sci. Rep.* **2017b**, *7*, 40318.
(14) Yue, S. J.; Xin, L. T.; Fan, Y. C.; Li, S. J.; Tang, Y. P.; Duan, J. A.; Guan, H. S.; Wang, C. Y. Herb pair Danggui-Honghua: mechanisms underlying blood stasis syndrome by system pharmacology approach. *Sci. Rep.* **2017b**, *7*, 40318.
(15) Yue, S. J.; Xin, L. T.; Fan, Y. C.; Li, S. J.; Tang, Y. P.; Duan, J. A.; Guan, H. S.; Wang, C. Y. Herb pair Danggui-Honghua: mechanisms underlying blood stasis syndrome by system pharmacology approach. *Sci. Rep.* **2017b**, *7*, 40318.
(16) Yue, S. J.; Xin, L. T.; Fan, Y. C.; Li, S. J.; Tang, Y. P.; Duan, J. A.; Guan, H. S.; Wang, C. Y. Herb pair Danggui-Honghua: mechanisms underlying blood stasis syndrome by system pharmacology approach. *Sci. Rep.* **2017b**, *7*, 40318.
(17) Yue, S. J.; Xin, L. T.; Fan, Y. C.; Li, S. J.; Tang, Y. P.; Duan, J. A.; Guan, H. S.; Wang, C. Y. Herb pair Danggui-Honghua: mechanisms underlying blood stasis syndrome by system pharmacology approach. *Sci. Rep.* **2017b**, *7*, 40318.
(18) Yue, S. J.; Xin, L. T.; Fan, Y. C.; Li, S. J.; Tang, Y. P.; Duan, J. A.; Guan, H. S.; Wang, C. Y. Herb pair Danggui-Honghua: mechanisms underlying blood stasis syndrome by system pharmacology approach. *Sci. Rep.* **2017b**, *7*, 40318.
(19) Yue, S. J.; Xin, L. T.; Fan, Y. C.; Li, S. J.; Tang, Y. P.; Duan, J. A.; Guan, H. S.; Wang, C. Y. Herb pair Danggui-Honghua: mechanisms underlying blood stasis syndrome by system pharmacology approach. *Sci. Rep.* **2017b**, *7*, 40318.
(20) Yue, S. J.; Xin, L. T.; Fan, Y. C.; Li, S. J.; Tang, Y. P.; Duan, J. A.; Guan, H. S.; Wang, C. Y. Herb pair Danggui-Honghua: mechanisms underlying blood stasis syndrome by system pharmacology approach. *Sci. Rep.* **2017b**, *7*, 40318.
(21) Yue, S. J.; Xin, L. T.; Fan, Y. C.; Li, S. J.; Tang, Y. P.; Duan, J. A.; Guan, H. S.; Wang, C. Y. Herb pair Danggui-Honghua: mechanisms underlying blood stasis syndrome by system pharmacology approach. *Sci. Rep.* **2017b**, *7*, 40318.
(22) Yue, S. J.; Xin, L. T.; Fan, Y. C.; Li, S. J.; Tang, Y. P.; Duan, J. A.; Guan, H. S.; Wang, C. Y. Herb pair Danggui-Honghua: mechanisms underlying blood stasis syndrome by system pharmacology approach. *Sci. Rep.* **2017b**, *7*, 40318.
(23) Yue, S. J.; Xin, L. T.; Fan, Y. C.; Li, S. J.; Tang, Y. P.; Duan, J. A.; Guan, H. S.; Wang, C. Y. Herb pair Danggui-Honghua: mechanisms underlying blood stasis syndrome by system pharmacology approach. *Sci. Rep.* **2017b**, *7*, 40318.
(24) Yue, S. J.; Xin, L. T.; Fan, Y. C.; Li, S. J.; Tang, Y. P.; Duan, J. A.; Guan, H. S.; Wang, C. Y. Herb pair Danggui-Honghua: mechanisms underlying blood stasis syndrome by system pharmacology approach. *Sci. Rep.* **2017b**, *7*, 40318.
(25) Yue, S. J.; Xin, L. T.; Fan, Y. C.; Li, S. J.; Tang, Y. P.; Duan, J. A.; Guan, H. S.; Wang, C. Y. Herb pair Danggui-Honghua: mechanisms underlying blood stasis syndrome by system pharmacology approach. *Sci. Rep.* **2017b**, *7*, 40318.
(26) Cantó, C.; Auwerx, J. PGC-1alpha, SIRT1 and AMPK, an energy sensing network that controls energy expenditure. *Curr. Opin. Lipidol.* **2009**, *20*, 98−105.
(27) Kim, D. E.; Chang, B. Y.; Jeon, B. M.; Baek, J. I.; Kim, S. C.; Kim, S. Y. SGL 121 attenuates nonalcoholic fatty liver disease through adjusting lipid metabolism through AMPK signaling pathway. *Int. J. Mol. Sci.* **2020**, *21*, 4534.
(28) Talagavadi, V.; Rapisarda, P.; Galvano, F.; Pelicci, P.; Giorgio, M. Cyanidin-3-O-β-glucoside and protocatechuic acid activate AMPK/mTOR/S6K pathway and improve glucose homeostasis in mice. *J. Funct. Foods* **2016**, *21*, 338−348.
(29) Huang, M. Q.; Zhou, C. J.; Zhang, Y. P.; Zhang, X. Q.; Xu, W.; Lin, J.; Wang, P. J. Salvianolic acid B ameliorates hyperglycemia and dyslipidemia in db/db mice through the AMPK pathway. *Cell. Physiol. Biochem.* **2016**, *40*, 933−943.
(30) Qiang, G.; Yang, X.; Shi, L.; Zhang, H.; Chen, B.; Zhao, Y.; Zu, M.; Zhou, D.; Guo, J.; Yang, H.; et al. Antidiabetic effect of salvianolic acid A on diabetic animal models via AMPK activation and mitochondrial regulation. *Cell. Physiol. Biochem.* **2015**, *36*, 395−408.
(31) Abe, D.; Saito, T.; Nogata, Y. Rosmarinic acid regulates fatty acid and glucose utilization by activating the CaMKK/AMPK pathway in C2C12 myotubes. *Food Sci. Technol. Res.* **2016**, *22*, 779−785.
(32) Meng, F.; Su, X.; Li, W.; Zheng, Y. Ginsenoside Rb3 strengthens the hypoglycemic effect through AMPK for inhibition of hepatic gluconeogenesis. *Exp. Ther. Med.* **2017**, *13*, 2551−2557.
(33) Lee, M. S.; Hwang, J. T.; Kim, S. H.; Yoon, S.; Kim, M. S.; Yang, H. J.; Kwon, D. Y. Ginsenoside Rc, an active component of *Panax ginseng*, stimulates glucose uptake in C2C12 myotubes through an AMPK-dependent mechanism. *J. Ethnopharmacol.* **2010**, *127*, 771−776.
(34) Ru, J. L.; Li, P.; Wang, J. N.; Zhou, W.; Li, B. H.; Huang, C.; Li, P.; Guo, Z.; Tao, W.; Yang, Y.; et al. TCMSP: a database of systems pharmacology for drug discovery from herbal medicines. *Aust. J. Chem.* **2014**, *6*, 1498−1504.
(35) Xu, X.; Zhang, W. X.; Huang, C.; Li, Y.; Yu, H.; Wang, Y. H.; Duan, J.; Ling, Y. A novel chemometric method for prediction of human oral bioavailability. *Int. J. Mol. Sci.* **2012**, *13*, 6964−6982.
(36) Ma, C.; Wang, L.; Xie, X. Q. GPU accelerated chemical similarity calculation for compound library comparison. *J. Chem. Inf. Model.* **2011**, *51*, 1521−1527.
(37) Daina, A.; Michielin, O.; Zoete, V. SwissTargetPrediction: updated data and new features for efficient prediction of protein targets of small molecules. *Nucleic Acids Res.* **2019**, *47*, W357−W364.
(38) Davis, A. P.; Grondin, C. J.; Johnson, R. J.; Sciaky, D.; McMorran, R.; Wiegers, J.; Wiegers, T. C.; Mattingly, C. J. The comparative toxicogenomics database: update 2019. *Nucleic Acids Res.* **2019**, *47*, D948−D954.
(39) Amberger, J. S.; Bocchini, C. A.; Schiettecatte, F.; Scott, A. F.; Hamosh, A. OMIM.org: Online Mendelian Inheritance in Man (OMIM), an online catalog of human genes and genetic disorders. *Nucleic Acids Res.* **2015**, *43*, D789−D798.
(40) Stelzer, G.; Rosen, N.; Plaschkes, I.; Zimmerman, S.; Twik, M.; Fishilevich, S.; Stein, T.; Nudel, R.; Lieder, I.; Mazor, Y.; et al. The GeneCards suite: from gene data mining to disease genome sequence analyses. *Curr. Protoc. Bioinformatics* **2016**, *54*, 1.30.1−1.30.33.

https://doi.org/10.1021/acsomega.1c01209
ACS Omega 2021, 6, 17276−17288

(41) Huang da, W.; Sherman, B. T.; Lempicki, R. A. Systematic and integrative analysis of large gene lists using DAVID bioinformatics resources. *Nat. Protoc.* **2009**, *4*, 44−57.
(42) Smoot, M. E.; Ono, K.; Ruscheinski, J.; Wang, P. L.; Ideker, T. Cytoscape 2.8: new features for data integration and network visualization. *Bioinformatics* **2011**, *27*, 431−432.
(43) Wang, T.; Streeter, H.; Wang, X.; Purnama, U.; Lyu, M.; Carr, C.; Ma, Y. L. A network pharmacology study of the multi-targeting profile of an antiarrhythmic Chinese medicine Xin Su Ning. *Front. Pharmacol.* **2019**, *10*, 1138.
(44) Zhao, X.; Hao, J.; Chen, S. Network pharmacology-based strategy for predicting therapy targets of traditional Chinese medicine Xihuang Pill on liver cancer. *Evid. Based Compl. Alt.* **2020**, *2020*, 1.
(45) Jiang, B.; Le, L.; Zhai, W.; Wan, W.; He, K.; Yong, P.; He, C.; Xu, L.; Xiao, P. Protective effects of marein on high glucose-induced glucose metabolic disorder in HepG2 cells. *Phytomedicine* **2016**, *23*, 891−900.
(46) Li, P.; Ding, L.; Cao, S.; Feng, X.; Zhang, Q.; Chen, Y.; Zhang, N.; Qiu, F. Curcumin metabolites contribute to the effect of curcumin on ameliorating insulin sensitivity in high-glucose-induced insulin-resistant HepG2 cells. *J. Ethnopharmacol.* **2020**, *259*, No. 113015.

https://doi.org/10.1021/acsomega.1c01209
ACS Omega 2021, 6, 17276−17288